Visualization of Space-Charge Waves in Photorefractive Semiconductor Using Polarimetric Technique

K. Shcherbin[1], V. Danylyuk[1] and A. Khomenko[2]

[1] Institute of Physics of NAS, 46 Prospekt Nauki, 03650 Kiev, Ukraine,
e-mail: kshcherb@iop.kiev.ua
[2] Centro de Investigación Científica y de Educación Superior de Ensenada, Km. 107 Carretera Tijuana-Ensenada, Ensenada, B.C. 22860, México

Received: 01.09.2006

Abstract

We suggest visualizing space-charge waves (SCW) in the near field in homogeneously illuminated photorefractive crystal, using modulation of optical polarization induced by the SCW due to the Pockels effect. Spatial distribution of SCW is obtained in the near field for a photorefractive semiconductor placed between polarizers. It is shown that the internal field in the crystal is not homogeneous, the SCW at different points are excited with different amplitudes and their structure is not perfectly regular. Qualitative agreement of existing theoretical model with our experimental data is demonstrated. Using the model, the mobility-lifetime product for the free carriers and the effective trap concentration are estimated.

Keywords: space-charge waves, photorefraction, cadmium telluride

PACS: 42.65.Hw; 42.70.Nq; 52.35.Mw; 72.80.Ey

Introduction

Space-charge waves (SCW) are a subject of extensive studies in different fields of physics, including plasma physics, physics of semiconductors and photorefraction. In photorefractive crystals, SCW are associated with the waves of spatial recharging of traps, which can be excited in the presence of electric field [1–3]. They are considered as eigen modes of a space-charge field with a certain spatial frequency (wavelength), eigen frequency and dumping constant determined by the crystal parameters and the field amplitude [2,3]. The stronger the external field, the lower the spatial frequency of the SCW (i.e., the larger the SCW wavelength) and the larger the amplitude of the SCW is. If the spatial frequency of the grating is close to that of the SCW, resonant excitation of the SCW takes place and the grating is increased considerably. Besides, if the spatial frequency of the grating is an integer fraction of that of the SCW, an exciting phenomenon of generation of spatial subharmonics occurs.

Optical excitation of SCW is used in experimental investigations that deal with recording of moving gratings in photorefractive crystals in the presence of dc field [3,4] or when stationary gratings are recorded in ac-biased crystals [3,5]. An elegant technique of oscillating interference pattern has also provided many interesting results [6]. All of these methods allow a selective excitation of SCW with the parameters depending on characteristics of recording light-induced grating. However, the SCW could be also excited in homogeneously illuminated crystals. Then they are excited with optimal spatial frequency and their spatial frequency spectrum may be relatively broad.

When being excited, the SCW result in refractive index grating, like any regular spatial charge redistribution in a photorefractive crystal.

That is why the SCW in photorefractive crystals are studied mainly by diffractive techniques, i.e., the diffraction from the SCW-related gratings is studied. These techniques enable one to measure overall characteristics of the SCW averaged over the cross-section of crystal.

In the present paper we propose and demonstrate a practical use of polarimetric technique for studies of spatial structure of the SCW. As with any electro-optic crystal, the space-charge field in a photorefractive crystal transforms into spatial refractive index modulation. This modulation results in diffraction from the space-charge grating, which is usually studied. On the other hand, this modulation may also give a spatial modulation of polarization of the light transmitted through the crystal. Similar effect has been widely used in spatial light modulators 'PROM' and 'PRIZ' [7]. Here we suggest utilization of the spatial polarization modulation for direct visualization of SCW structure in the near field. The technique has allowed us visualizing successfully the SCW in CdTe, to study its spatial structure and estimate some crystal parameters such as the mobility-lifetime product for the majority charge carriers and the density of effective traps.

Experiment

Germanium-doped CdTe crystal was used in our experiments. Generation of spatial subharmonics reported for this particular sample (see [8]) confirms that the SCW are excited under definite conditions. The crystal was grown by Bridgman technique in Chernivtsy National University, Ukraine. It was deliberately doped with germanium and exhibited dark conductivity of the order of 10^{-9} $(\Omega\,\mathrm{cm})^{-1}$. The single-crystal sample was cut along $[11\bar{2}]$, $[111]$ and $[1\bar{1}0]$ crystallographic axes. It had the dimensions $4\times4.4\times9.6$ mm^3, whose sequence corresponds to that of the mentioned crystallographic directions. The input and output faces parallel to crystallographic plane $(1\bar{1}0)$ were optically polished. The electrodes were deposited with a silver paste on the side faces parallel to (111) plane. Nearly square-shaped ac voltage, with the frequency f = 700 Hz and the amplitude up to 4 kV, was applied to these faces, thus forming an internal field E_{in} along [111] axis. We mark this axis as z further on. The slew rate of the high-voltage generator was greater than 200 V/μs, so that quite good square waveform could be obtained at the frequency of 700 Hz.

Schematic representation of our experimental set-up is shown in Fig. 1. The expanded output beam of a single-mode single-frequency diode-pumped Nd^{3+}:YAG laser (the wavelength 1.064 μm) illuminated CdTe crystal through $(1\bar{1}0)$ plane. The crystal was placed between polarizer and analyser, which transmitted light with parallel polarizations. In case of our sample, this orientation of polarizer and analyzer ensured better contrast of the pictures on CCD-camera, when compare to the crossed arrangement. The angle between the light polarization vector and [111] axis of the crystal was 45°. The intensity of the input beam I_{in} on the input sample face was about 20 mW/cm^2, with less than 10%-variation over the whole cross-section. The image of the back sample face was transferred to CCD camera SONY CV-235 by a lens with 12.5 cm focal length. A diaphragm D was placed just in front

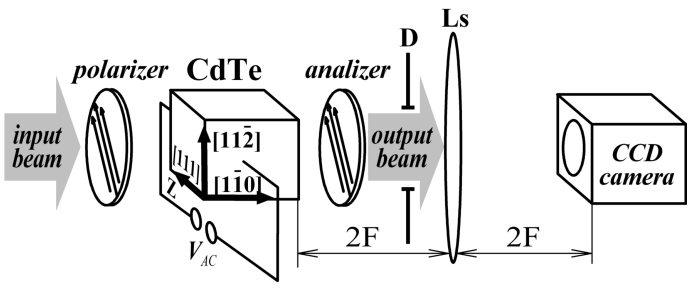

Fig. 1. Schematic representation of experimental setup. D is a diaphragm and Ls a lens with focal distance F.

of the lens, in order to transmit the entire transmitted beam though reduce the amount of the scattered light and the light diffracted from the SCW that might fall onto the CCD camera.

The system polarizer-crystal-analyzer is nothing but a simple amplitude electro-optic modulator. If there are no screening effects in crystal, the negative and positive half-periods produce similar intensity changes for the output beam. Since the frequency of the applied field is much higher than the sampling frequency of the CCD camera, the CCD records the time-averaged intensity distribution, which should be the same, though for the negative and positive half-periods of the external voltage.

The pictures recorded by the CCD camera at different amplitudes of the applied voltage are shown in Fig. 2. The intensity is maximal if no field is applied (Fig. 2a), since CdTe has a cubic symmetry and does not rotate polarization of light. The sample image is nearly homogeneous. The horizontal fringes observed over the whole sample are caused by multiple reflections from the output and input surfaces, which are not parallel. Besides, a few defects of surface polishing are visible. However, no vertical structure is observed.

The transmitted light intensity changes when the voltage is applied, since the electric field introduces some ellipticity to the light polarization. These changes are not homogeneous along [111] direction (see Fig. 2b). A large-scale inhomogeneity is caused by spatial inhomogeneity of the resistance of crystal and, as a result, nonuniformity of the electric field inside the crystal. This effect will be discussed further on. When the external voltage V_{AC} exceeds 1.8 kV, nearly regular fringes with the spatial period of about 100 μm become visible in the middle part of the sample (see Fig. 2c). These fringes occupy nearly the whole backside of the crystal when the voltage increases still more, the contrast of the fringes gets higher, while the spatial period increases (see Fig. 2d). When the analyzer is removed

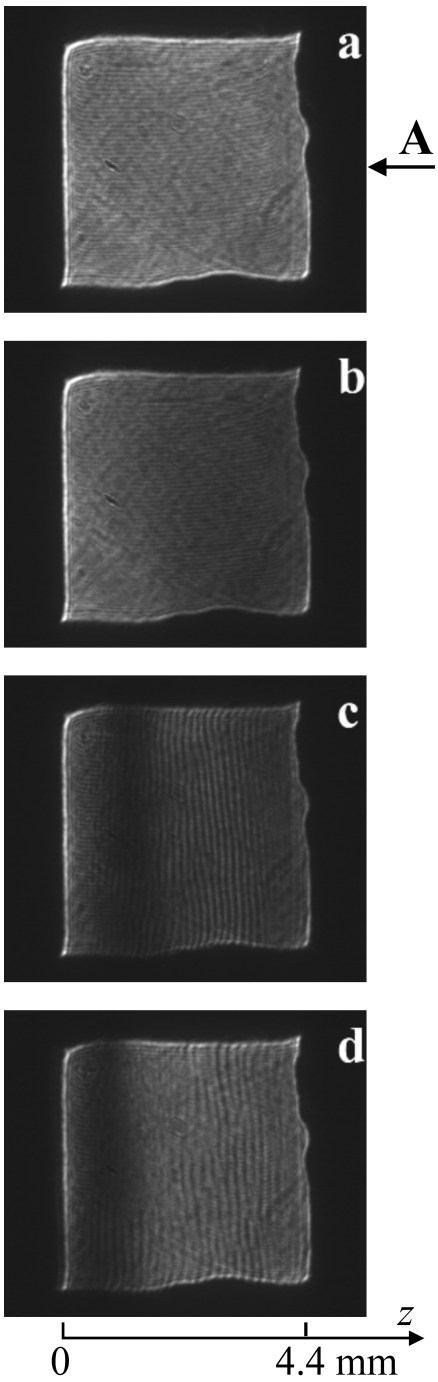

Fig. 2. The intensity distribution behind the crystal observed at different amplitudes of the applied ac voltage: a – 0, b – 1.2, c – 2.8 and d – 3.6 kV.

from the set-up, the picture of the backside is always homogeneous and similar to that presented in Fig. 2a, irrespective of the applied voltage. The intensity modulation is therefore caused by the modulation of light polarization behind the crystal. The internal field in the crystal includes the component due to SCW, which

introduces spatial modulation of the light polarization. The intensity modulation observed behind the polarizer (with the spatial period of the order of 100 μm) repeats this modulation and demonstrates the structure and redistribution of the SCW occurring in the CdTe crystal under study.

Discussion

The proposed polarimetric technique allows one to visualize in the near field the SCW excited in photorefractive CdTe. The structure of the SCW becomes visible, which can be never reached with traditional diffractive methods used before for the studies of SCW. With our optical polarization technique, it becomes immediately evident that the SCW are not excited over the whole cross-section of crystal and the amplitude is different at different points. The structure of the SCW is not perfectly regular and manifests the edge points and dislocations.

Apart of the SCW structure, the polarimetric technique also enables studying some their properties. The data of Fig. 2 can be presented as optical transmittance of the set-up at any point of the sample cross-section:

$$T = I_{TR} / I_{TR}^{0}, \qquad (1)$$

where I_{TR} and I_{TR}^{0} are the light intensities transmitted at the same point of sample backside behind the analyzer, which are related respectively to the applied voltage V_{AC} and no voltage. The transmittance of the optical system for a middle section of the backside along [111] direction, which is marked as A in Fig. 2, is presented in Fig. 3 for different applied voltages. We can easily estimate from Fig. 2 the wavelength of the SCW at different points of crystal under different applied voltages.

On the other hand, the transmittance of the optical system with polarizers oriented so as to transmit the light with the same polarizations can be written as

$$T = \cos^2 \frac{\Phi}{2}, \qquad (2)$$

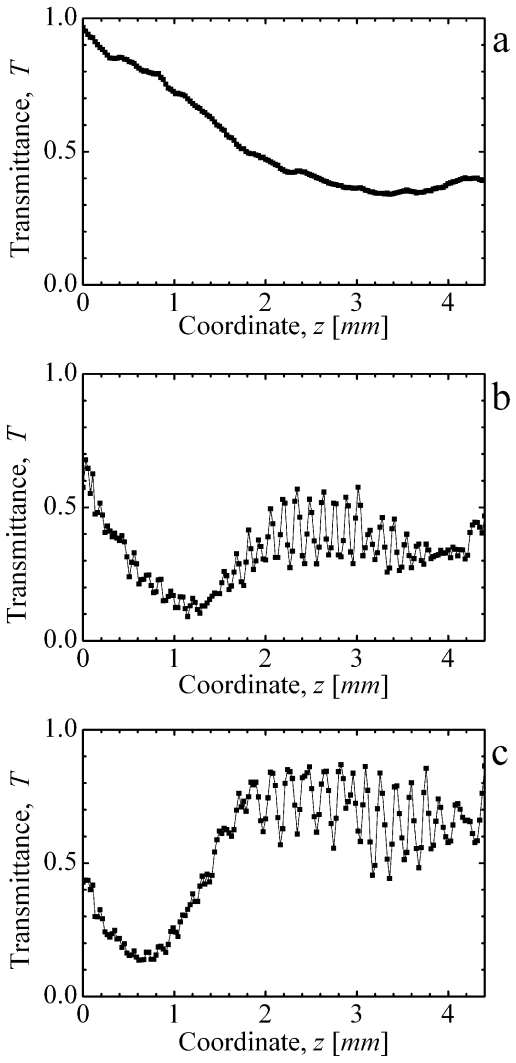

Fig. 3. Transmittance distribution of the system polarizer-crystal-analyzer along z axis for different amplitudes of the applied ac voltage: a – 1.2, b – 2.8 and c – 3.6 kV.

where

$$\Phi = \frac{2\pi(n_e - n_o)L}{\lambda} \qquad (3)$$

is the phase difference between the light components polarized extraordinarily (along [111] axis) and ordinarily (perpendicular to this axis) upon passing the crystal, n_e and n_o are the refractive indices for these components in the presence of external voltage, L is the sample length and λ the light wavelength. The refractive index is isotropic for cubic crystals with no external field, i.e., $n_o = n_e$ if $E_{in} = 0$. When the external field is applied to crystals of $\bar{4}3m$ symmetry group along [111] direction, like in

our case, the refractive indices n_o and n_e are the main ones and are defined as (see, e.g., [9])

$$\begin{aligned} n_o &= n - \frac{1}{\sqrt{3}} n^3 r_{41} E_{in} \\ n_e &= n + \frac{1}{2\sqrt{3}} n^3 r_{41} E_{in} \end{aligned}, \qquad (4)$$

with r_{41} being the electro-optic constant well known from handbooks. Using Eqs. (2)–(4) and the transmittance distribution, one can easily find the electric field in the crystal along z axis:

$$E_{in}(z) = \frac{2\lambda \arccos\sqrt{T(z)}}{\sqrt{3}\pi n^3 r_{41} L}. \qquad (5)$$

Indeed, the electric field may be then found as a function of both coordinates measured along [111] and [11$\bar{2}$] crystallographic directions.

The electric field profile in our crystal is shown in Fig. 4 for different applied voltages. There is a large data scattering in the literature concerning the electro-optic constant of CdTe. When estimating the electric field, we have used r_{41} = 6.1 pm/V [10], which is the most reliable, according to our rough experimental estimations performed on different crystals at λ = 1.06 μm. The spatial modulation of the internal field is clearly seen in Fig. 4. The amplitude of the SCW increases with increasing field and reaches the amplitude of about 800 V/cm if the voltage ~ 4 kV/cm is applied. The wavelength of the SCW also increases with increasing field and exceeds 200 μm under large fields. It is also seen that the mean field E_M is not uniform in the crystal. Let us discuss this difference now.

When a dc voltage is applied to the crystal, the internal electric field follows after the resistivity distribution. However, the field would remain homogeneous, if the ac voltage of high frequency is applied, at which the imaginary impedance is much smaller than the resistive impedance:

$$\frac{1}{2\pi f C} << R, \qquad (6)$$

where C is the capacity and R the resistance of crystal.

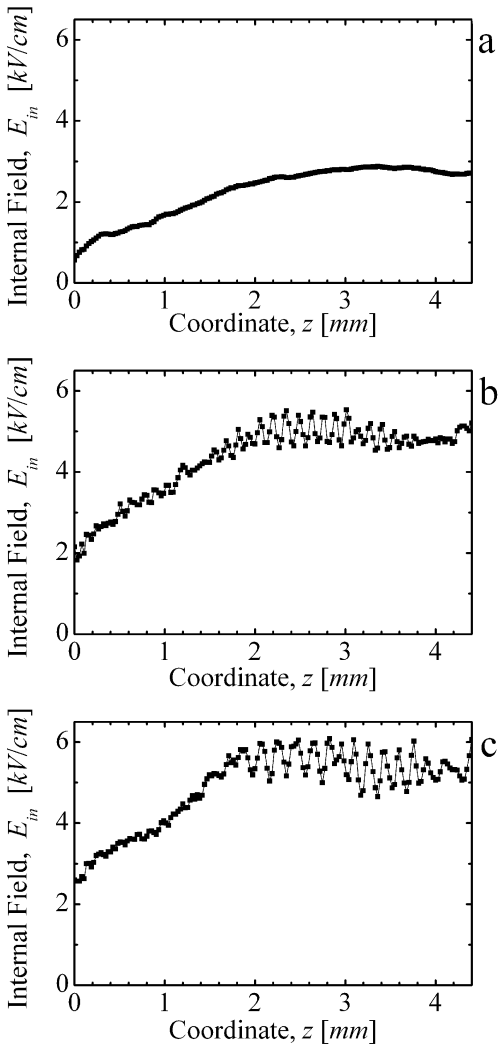

Fig. 4. Distribution of the internal field in crystal that occurs along z axis for different amplitudes of the applied ac voltage: a – 1.2, b – 2.8 and c – 3.6 kV.

Nonuniformity of the mean field indicates that the active resistance is still important at the frequency f = 700 Hz used in the experiments. We have made the experimental estimation R = 40 MΩ and have calculated that C = 0.7 pF, using the dimensions of our sample. With these quantities, the reactance of crystal would become equal to the resistive impedance only at the frequency ~ 5.7 kHz. It is very difficult technical task to provide such high-frequency high voltage. The power supply we utilize in the present studies cannot produce the fields of this kind. It is known, however, that the response time of photorefractive gratings is larger than the dielectric time constant of the material at

finite grating spacing and it increases in the presence of external electric field [5,7]. Therefore, even a relatively low frequency we use may be sufficiently high for the SCW grating and the field may be regarded as ac one. So, the technique of excitation of the SCW should be considered as quasi-ac technique.

However, the excitation method is not crucially important if we deal with demonstration of the visualization technique for the SCW. Moreover, the proposed technique has enabled one to show that the mean electric field is not homogeneous in the crystal. This nonuniformity is caused by inhomogeneity of the active resistance, which is inherent to the crystals under test. Unfortunately, nonuniformity of the properties is habitual for CdTe, because of difficulties with the synthesis techniques for single crystals. Further improvement of the crystal growth technique is necessary, which can really yield breakthrough in the industrial applications of CdTe.

Let us also notice that, for large enough applied voltage exceeding 2.5 kV, the internal field in the crystal evaluated on the basis of the technique suggested here does not reach the value that should be true for the case of the homogeneous distribution ($E = V/d$, where d is the distance between electrodes). Most probably, this is caused by the contact effect known for CdTe [11].

In homogeneously illuminated crystal, the SCW are excited at optimal spatial frequency, for which the quality factor of SCW is maximal. This optimal frequency is determined as [3]

$$\frac{1}{K_{opt}} = \sqrt{\frac{\mu\tau k_B T}{e}\left(1 + E_{in}^2 \frac{\varepsilon\varepsilon_0}{N_E k_B T}\right)}, \qquad (7)$$

where $\mu\tau$ is the mobility-lifetime product for free carriers, k_B the Boltzmann constant, T the absolute temperature, e the electron charge, N_E the effective trap density and ε and ε_0 are respectively the dielectric constants of the material and vacuum. We can measure in the experiment the SCW wavelength $\Lambda = 2\pi/K$. It is therefore convenient to rewrite Eq. (7) as a function of Λ:

$$\Lambda = 2\pi\sqrt{\mu\tau\frac{k_B T}{e}\left(1 + E_{in}^2 \frac{\varepsilon\varepsilon_0}{N_E k_B T}\right)} = 2\pi l_D \sqrt{1 + E_{in}^2 \frac{\varepsilon\varepsilon_0}{N_E k_B T}}, \qquad (8)$$

where $l_D = \sqrt{\mu\tau\frac{k_B T}{e}}$ is the diffusion length of free carriers.

Since the crystal is inhomogeneous and the internal field nonuniform, we have selected the area in the crystal located between z = 0.25 cm and z = 0.32 mm and studied the dependence of SCW wavelength on the field in this area. The experimental dependence is represented in Fig. 5 by full squares as a function of mean field E_{in} in the selected interval of z (it is assumed that E_{in} = const in this interval). The theoretical model predicts that the SCW wavelength increases linearly at large fields, when we can neglect the unity appearing in the brackets in Eq. (8). The ratio $\mu\tau/N_E \approx 5\times10^{-30}$ m^5/V is estimated from the slope of the experimental dependence in Fig. 5. For low fields, the component in the brackets containing E_{in} can be ignored. Then the SCW wavelength would be defined mainly by the diffusion length. A rough estimate could be made that the diffusion length is definitely 2π times smaller than the lowest detected SCW wavelength, i.e., $l_D < \Lambda_{min}/2\pi$ = 13 μm. Of course, one should note that the SCW are not excited under a zero field. Taking into account the estimates made above, we can ascertain that $\mu\tau < 6.5\times10^{-9}$ m^2/V and $N_E < 1.3\times10^{21}$ m^{-3}. The dashed curve in Fig. 5 is calculated using Eq. (8) and involving these limiting crystal characteristics. The solid line represents the dependence calculated with $\mu\tau = 2\times10^{-10}$ m^2/V and $N_E = 4.5\times10^{19}$ m^{-3}. Though a set of the fitting parameters may be modified, a perfect qualitative agreement of our experimental data with the theory is obvious.

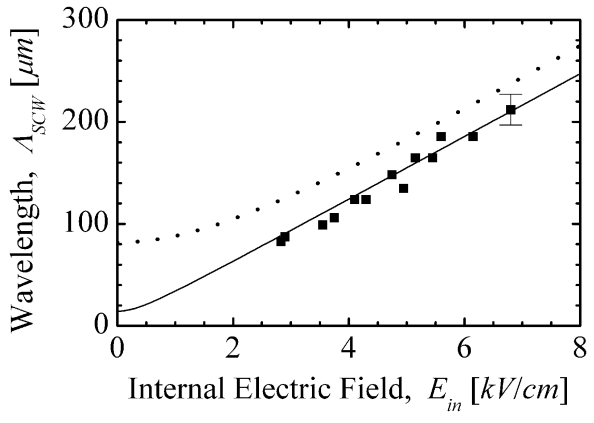

Fig. 5. SCW wavelength as a function of internal electric field: squares are experimental data and lines are calculated according to Eq. (8), with $\mu\tau = 6.5\times10^{-9}$ m^2/V and $N_E = 1.3\times10^{21}$ m^{-3} (dashed line) and $\mu\tau = 10^{-10}$ m^2/V and $N_E = 4.5\times10^{19}$ m^{-3} (solid line).

Conclusions

In the present paper we demonstrate that the changes in the light polarization induced by the SCW field can be used for direct visualisation of its structure in the near field. Excellent qualitative agreement between the theoretical model for SCW excitation and the experimental data is reached. Using this model, we have evaluated the ratio of the mobility-lifetime product for the free carriers and the effective trap concentration. The mobility-lifetime product and the effective trap concentration themselves are also estimated.

Certainly, the technique of lens transfer may be used for visualization in the near field of spatial structure of any grating recorded in any media. For this aim, all the diffracted orders should be transposed on a recording medium like a CCD camera. The interference of all the diffracted orders would reconstruct a spatial structure of the diffraction grating.

Acknowledgements

K. Shcherbin cordially thanks his colleagues from Optical Department of CICESE for their hospitality. A. V. Khomenko acknowledges a support from Consejo Nacional de Ciencia y Tecnología, México, under the project 44006. The authors are grateful to Z. Zakharuk and I. Rarenko for supplying CdTe sample.

References

1. Kazarinov R. F., Suris R. A. and Fuks B. I. Sov. Phys. Semicond. **7** (1973) 102.
2. Sturman B., Bledowski A., Otten J. and Ringhofer K. J. Opt. Soc. Am. B **10** (1993) 1919.
3. Sturman B. I. Space-charge wave effects in photorefractive materials. In "Photorefractive materials and their applications I". New York, Springer Science + Business Media, Inc. (2006) 119.
4. Huignard J. P. and Marrakchi A. Opt. Commun. **38** (1981) 249.
5. Stepanov S. I. and Petrov M. P. Opt. Commun. **53** (1985) 292.
6. Petrov M. P., Paugurt A. P., Bryksin V. V., Wevering S. and Krätzig E. Phys. Rev. Lett. **84** (2000) 5114.
7. Petrov M. P., Stepanov S. I. and Khomenko A. V. Photorefractive crystals in coherent optical systems. Berlin, Springer-Verlag (1991).
8. Shcherbin K. Appl. Phys. B **71** (2000) 123.
9. Yariv A. and Yeh P. Optical waves in crystals. New York, Wiley (1984).
10. Tada K. and Aoki M. Jpn. J. Appl. Phys. **10** (1971) 998.
11. Ziari M. and Steier W. H. Appl. Opt. **32** (2002) 5711.